

Fundamental Understanding of the Di-Air System: The Role of Ceria in NO_x Abatement

Yixiao Wang¹ · Jorrit Posthuma de Boer¹ · Freek Kapteijn¹ · Michiel Makkee¹

Published online: 4 May 2016

© The Author(s) 2016. This article is published with open access at Springerlink.com

Abstract Temporal analysis of product (TAP) is used to investigate the effectiveness of CO, C₃H₆, and C₃H₈ in the reduction of a La–Zr doped ceria catalyst and NO reduction into N₂ over this pre-reduced catalyst. Hydrocarbons are found to be substantially more effective in the reduction of this catalyst at high temperature (above 500 °C) as compared to CO. NO decomposes over oxygen anion defects created upon catalyst reduction. Deposited carbon, in case the catalyst is reduced by C₃H₆ or C₃H₈, acts as a delayed or stored reductant and is not directly involved in NO reduction. Instead the oxidation of deposited carbon by an oxygen species derived from lattice oxygen (re)creates the oxygen anion defects active in NO reduction. In situ Raman, in which NO is flown over C₃H₆ pre-reduced La–Zr doped ceria at 560 °C, additionally shows that re-oxidation of the La–Zr doped ceria catalyst starts prior to the oxidation of deposited carbon, which confirms our TAP findings that firstly NO re-oxidized the La–Zr doped ceria catalyst and that secondly the oxidation of deposited carbon only commences at a higher ceria oxidation state. These findings create a new perspective on the operating principle of Toyota's Di-Air system.

Keywords NO reduction · Di-air · Ceria · TAP · Hydrocarbon oxidation

1 Introduction

Customer demand and legislation, e.g., the introduction of mandatory CO₂ emission targets of 95 g/km by the year 2020 in the EU for the complete model range of car manufacturers, drives the development of more fuel efficient cars. Introduction of the current Euro 6 emission standard has seen the development of highly efficient lean-burn turbo-charged gasoline engines and catalytic deNO_x systems (Urea-Selective Catalytic reduction (SCR) and Lean NO_x Traps (NSR)) for the diesel engines. Euro 7 is anticipated to involve a further reduction of the NO_x emissions to 0.04 g/km, while particulate matter emissions remain at 0.005 g/km. In addition, the more realistic Worldwide Harmonized Light Vehicles Test Procedures (WLTP) is expected to replace the outdated and non-realistic New European Driving Cycle (NEDC).

The composition of diesel engine exhaust gas is approximately 200 ppm NO, 5 % CO₂, 5 % O₂, 4 % H₂O. To meet the future Euro 7, it is anticipated that this small concentration of NO has to be further reduced to 10 ppm in the competing presence of O₂, CO₂, and H₂O. To meet the Euro 7 standard new technologies may be required. The three-way catalyst (TWC) works efficiently under stoichiometric conditions and loses its activity in the presence of oxygen. Urea-SCR has a complex dosing system and might be too voluminous to fit into most of the small passenger diesel cars. The NSR still needs further improvement to achieve high NO_x conversion at higher temperatures and space velocity. Recently, Bisaiji et al. (Toyota Company) developed the Di-Air system in which short fuel rich and long fuel lean periods are created by a direct injection of fuel into the exhaust upstream of a NSR catalyst (Pt/Rh/Ba/K/Ce/Al₂O₃) [1, 2]. By using the same amount of fuel the optimal NO_x reduction was achieved

✉ Michiel Makkee
m.makkee@tudelft.nl

¹ Catalysis Engineering, Chemical Engineering Department,
Delft University of Technology, Julianalaan 136,
2628 BL Delft, The Netherlands

when large fuel injection pulses were used as compared to small fuel injection pulses and/or post injection directly into the engine. The Di-Air system can retain high NO_x conversion (above 80 %) up to 800 °C and, therefore, could be a promising technology to meet the future NO_x emission standards under realistic driving test conditions. The unique performance of this system is ascribed to the formation of stable isocyanate and isocyanide intermediates on the catalyst surface evidenced by FTIR observations at 250 °C [2, 3]. How this system can achieve this performance remains largely unresolved. In order to further develop and optimize this system, we started a detailed investigation into the operating principle of the Di-Air system. Initially we will primarily use the TAP technique (a vacuum pulse-response technique) [4] to investigate what the role of each Di-Air catalyst component.

Ceria is well-known as an important ingredient in automotive emission control, e.g., TWC, NSR catalyst, and active soot filters [5, 6] due to ceria's ability to rapidly and reversibly change oxidation state: $\text{Ce}^{4+} + \text{e}^- \leftrightarrow \text{Ce}^{3+} + \square$ (\square represents an oxygen anion vacancy). Depending on the oxidative or reductive nature of the atmosphere, it acts as an oxygen buffer, but in principle also as an oxidiser or reductant. A lot of fundamental reports on soot oxidation by using ceria base catalyst, although the origination of the active oxygen species for soot oxidation remains controversy [7, 8].

To study the role of the ceria component in Di-Air system we selected a commercial La–Zr doped ceria catalyst for its thermal stability [9]. Surprisingly, this catalyst turned out to be capable of performing all tasks required for an effective automotive emission reduction catalyst, fuel (HC hydrocarbon) oxidation, CO oxidation, and NO_x reduction. Here, we present the results of the reduction–oxidation behaviour of the La–Zr doped ceria catalyst, using CO, C_3H_6 , and C_3H_8 in the absence of gas-phase oxygen and its re-oxidation by NO. The performed experiments provide a clear picture of the product evolution as a function of the oxidation state of the catalyst.

2 Experimental

The BET surface area of the catalyst is determined by N_2 adsorption using a Tristar II 3020 Micromeritics outgassing after 16 h outgassing at 200 °C. Inductive coupling plasma-optical emission spectrometer (ICP-OES, PerkinElmer Optima 5300) is applied to obtain the catalyst composition. The surface composition of the catalyst is measured by the X-ray photoelectron spectroscopy (XPS, K-alpha Thermo Fisher Scientific spectrometer). Powder X-ray diffraction (XRD) was recorded by using Bruker-AXS D5005 with Co $K\alpha$ source. In-situ Raman spectra

(Renishaw, 2000) were recorded using a temperature controlled in situ Raman cell (Linkam, THMS 600). Ten scans were collected for each spectrum in the 100–4000 cm^{-1} range using continues grating mode with a resolution of 4 cm^{-1} and scan time 10 s. The spectrometer was calibrated daily using a silicon standard with a strong band at 520 cm^{-1} .

The main technique used in the study is on a home-made advanced temporal analysis of products (TAP). TAP is a vacuum pulse-response technique. Reactant gas pulses are introduced to a small finite volume upstream of a packed catalyst bed. These introduced reactant molecules and eventually formed products upon interaction with the catalyst diffuse through the packed catalyst bed until they leave the packed bed, where they are recorded versus time (response) by a mass spectrometer. TAP experiments were performed using 21.2 mg of the La–Zr doped ceria (BASF) catalyst packed between two quartz particle beds in the temperature range 200–600 °C. In all experiments a starting pulse size of approximately 1.6×10^{15} molecules was used, the pulse size gradually decreases during an experiment as the reactant is pulsed from a constant calibrated volume. Prior to an NO (20 vol. % in Ar, internal standard) or ^{15}NO pulse experiment: (1) the catalyst was oxidized using an O_2 (20 vol% in Ar) pulse train; (2) a pre-reduction using either CO (80 vol% in Ar), C_3H_6 (20 vol% in Ne) or C_3H_8 (20 vol% in Ne) pulses was performed until the product distribution did not change.

The hypothetical ceria layers concept is introduced in order to obtain insight in the reactivity of the actual surface as a function of the degree of reduction (surface oxidation state). As the ceria (111) crystal plane is a stoichiometric O–Ce–O tri-layer stacked along the [111] direction, we regard each O–Ce–O tri-layer as one hypothetical ceria layer (0.316 nm). Assuming a perfect cubic crystal structure (size 5.0 nm), the total amount of hypothetical ceria layers was determined to be 16 (111) layers. The total number of hexagonal surface units (Fig. 1) on the (111) surface is calculated to be $3.6 \cdot 10^{18}$ using the following equation:

$$N = \frac{S_{\text{BET}} \times W_{\text{sample}}}{S_{\text{hexagonal unit}}}$$

where the S_{BET} is 65 m^2/g , W_{sample} is 21.2 mg, $S_{\text{hexagonal}}$ of the hexagonal surface unit is 0.38 nm^2 .

The total amount of O in each crystal layer can be calculated to be $2.2 \cdot 10^{19}$ using the following equation:

$$N_{\text{Total O}} = N \times n$$

where the n represents the number of oxygen atoms in one hexagonal unit. As shown in Fig. 1, the number of oxygen atoms one hexagonal unit is 6. Assuming that Zr and La are Ce, a maximum of 25 % of the number of O ions in each

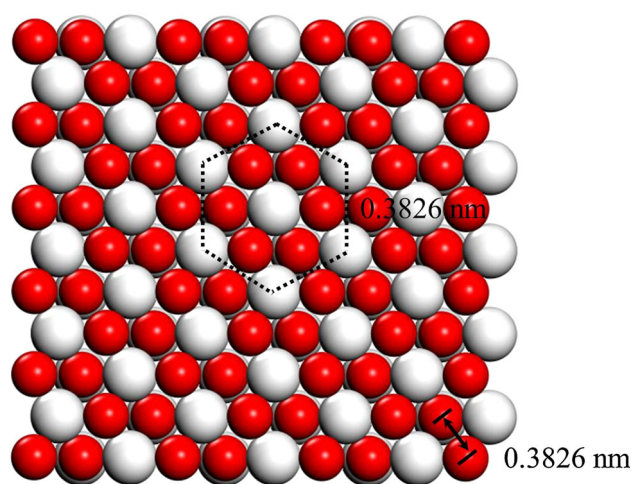


Fig. 1 Top view of the (111) crystal plane

crystal layer can be reduced, the amount of reducible oxygens in one hypothetical ceria layer is calculated to be $5.4 \cdot 10^{18}$.

3 Results and Discussion

3.1 Catalyst Characterization

The BET surface area of the La–Zr doped ceria is $65 \text{ m}^2/\text{g}$. The bulk composition of the La–Zr doped ceria sample is $\text{Ce}_{0.22}\text{Zr}_{0.07}\text{La}_{0.05}\text{O}_{0.66}$, as determined by inductively coupled plasma mass spectrometry (ICP). According to XPS, the surface ratio of Ce, Zr, and La is 170:92:1. Compared to the bulk composition the surface is enriched in Zr and there is hardly any La on the surface. XRD patterns (Fig. 2) shows the cubic structure, the crystal size is 5.0 nm based on the Scherrer equation;

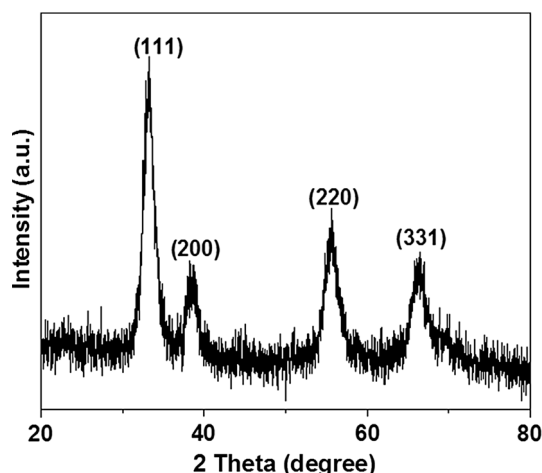


Fig. 2 XRD pattern of fresh La–Zr doped ceria

$$D = \frac{K\lambda}{\beta \cos \theta}$$

where λ is X-ray wavelength 0.1789 nm, K is the particle shape factor 0.94, and β is the full width at half height of the (111) peak.

3.2 Comparison of Reductant Activity Over the La–Zr Doped Ceria

In order to investigate the effectiveness of CO , C_3H_6 , and C_3H_8 in the reduction of the La–Zr doped ceria catalyst, CO , C_3H_6 , and C_3H_8 TAP pulse experiments were carried out, the obtained results are shown in the Figs. 3 and 4.

As shown in Fig. 3, until 0.4 reduced catalyst layers, CO is essentially completely converted to CO_2 . After this period CO conversion and CO_2 production progressively decrease, but never reaching a zero level during the duration of the experiment. The total amount of consumed oxygen atoms during the whole CO pulse experiment at 580°C is $6.3 \cdot 10^{18}$, i.e., CO can only reduce the catalyst to approximately 1.2 layers. Below 200°C , CO shows negligible activity in the reduction of ceria.

Figure 4a shows the result of a TAP single pulse experiment using C_3H_6 as a reductant over a pre-oxidized La–Zr doped ceria at 580°C . In phase I, up to 0.25 reduced catalyst layers, a high activity is observed where predominantly total oxidation products, i.e., CO_2 and H_2O are formed. H_2 formation is observed from the start of the experiment, while CO production is initially zero. H_2 as well as CO production increases during this phase I. In phase II the C_3H_6 conversion rapidly declines. In phase III pre-dominantly partial oxidation takes place and CO and H_2 are observed. In phase II and III the C_3H_6 conversion is low with exponentially increasing H_2 and CO production, but in phase IV, corresponding to 1.5–2.7 reduced catalyst layers, the C_3H_6 conversion increases to full conversion. In

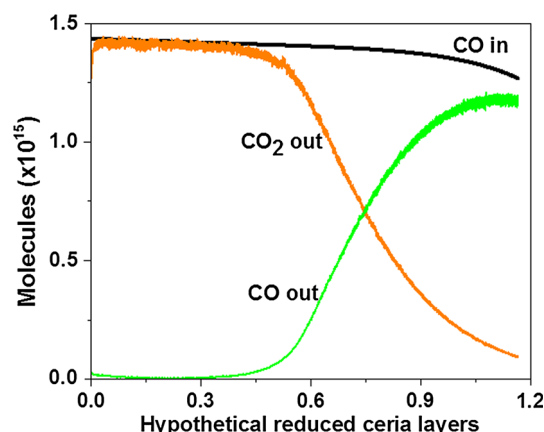
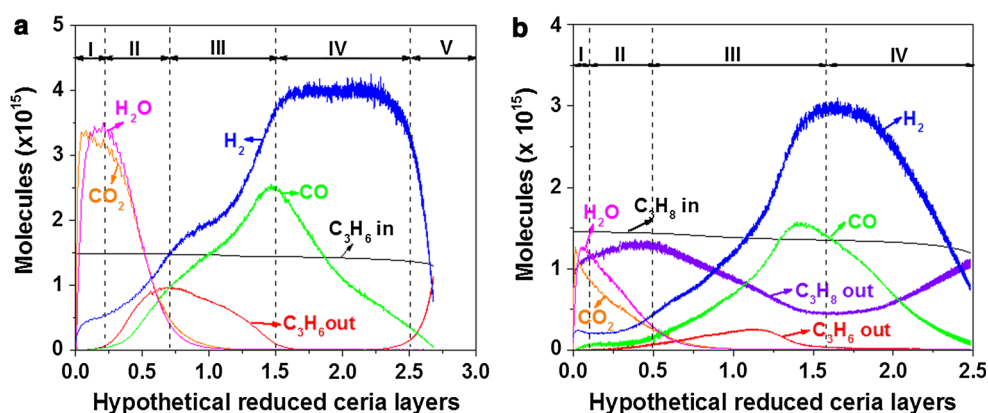


Fig. 3 CO pulses over pre-oxidised catalyst at 580°C

Fig. 4 **a** C_3H_6 pulses and **b** C_3H_8 pulses over pre-oxidised catalyst at 580 °C



phase V, when the ceria is reduced to more than 2.5 layers, C_3H_6 conversion and H_2 production decline. H_2 production remains persistent even when no CO is observed to evolve. Some carbon (determined from the carbon mass balance) starts to deposit over the surface when CO evolution is observed (phase II). Large amounts of carbon deposition are observed when the CO formation declines while H_2 formation persists (phase IV). C_3H_6 can reduce the catalyst as far as 2.7 layers and deposits $3.1 \cdot 10^{19}$ carbon atoms on the surface. Below 400 °C C_3H_6 shows negligible activity in ceria reduction and carbon deposition.

Figure 4b shows the result of a TAP single pulse experiment using C_3H_8 (model saturated hydrocarbon) as a reductant over pre-oxidized La–Zr doped ceria at 580 °C. In phase I, predominantly total oxidation products, i.e., CO_2 and H_2O are formed. H_2 formation is observed from the start of the experiment, while CO production is initially zero. H_2 as well as CO production increases during this phase I. C_3H_8 conversion declines in phase II and increases again during phase III. During phase II and III, partial oxidation takes place and CO, H_2 and C_3H_6 are observed. The C_3H_8 conversion over the whole experiment is substantially lower as compared to that of C_3H_6 . In phase IV, when the ceria is reduced to more than 1.5 layers, C_3H_8 conversion and H_2 production decline. H_2 production remains persistent even when no CO is observed to evolve. Some carbon (carbon mass balance) starts to deposit on the surface, when CO evolution is observed (phase I). Large amounts of carbon deposition are observed when the CO formation declines while H_2 formation persists (phase IV). C_3H_8 can reduce the catalyst up to 2.5 layers and deposits $1.5 \cdot 10^{19}$ carbon atoms on the surface. Below 500 °C C_3H_8 shows negligible activity in ceria reduction and carbon deposition. In general compared to CO, C_3H_6 , and C_3H_8 , C_3H_6 is more effective in the reduction of the catalyst at 580 °C.

During the CO pulse experiments, Ce^{4+} is reduced to Ce^{3+} , whereby oxygen anion defect sites are created, as

evidenced by the consumption of lattice oxygen atoms. While during the hydrocarbon pulse experiments, both the reduction of Ce^{4+} to Ce^{3+} and the deposition of carbon are observed. High hydrocarbon activity is observed both at low reduction state (number of reduced layers: 0–0.25) and at high reduction state (number of reduced layers: 1.5–2.7). The high activity at low reduction state is probably due to the existence and/or formation of active surface oxygen species (superoxide, O_2^- , and peroxide, O_2^{2-} ,) on the catalyst surface, as this surface oxygen species is reported to be responsible for total oxidation [10]. The surprising high activity at high reduction is probably due to the Ce^{3+} species with their associated oxygen anion defect. Oxygen anion defect sites can strongly bind adsorbates and assist in their dissociation [11]. Unsaturated hydrocarbon (C_3H_6) displays a higher reactivity as compared to the saturated hydrocarbons (C_3H_8), that is probably due to the weaker C–H bond strength of unsaturated hydrocarbons [12]. As compared to C_3H_6 and C_3H_8 , CO has a higher catalyst reduction ability at lower temperature, but it cannot compete with the reduction potential of hydrocarbons at temperatures above 500 °C.

3.3 NO Reduction Over the Pre-reduced La–Zr Doped Ceria by CO and Hydrocarbons

In order to investigate the roles of different reductants in the reduction of NO into N_2 over the La–Zr doped ceria catalyst, NO is pulsed over CO and C_3H_6 pre-reduced La–Zr doped ceria. Figure 5 displays the obtained results for the CO pre-reduced sample at 540 °C. Full NO conversion is obtained, while N_2 is the only product for 1.2–0.5 hypothetical reduced ceria layers. After that, NO conversion starts declining, accompanied by a parallel decrease in the N_2 production. The amount of oxygen atoms taken up by the catalyst during the NO pulse experiment is around $6.6 \cdot 10^{18}$, which is similar to the total oxygen atom consumption during the CO pre-reduction at 540 °C. Initially

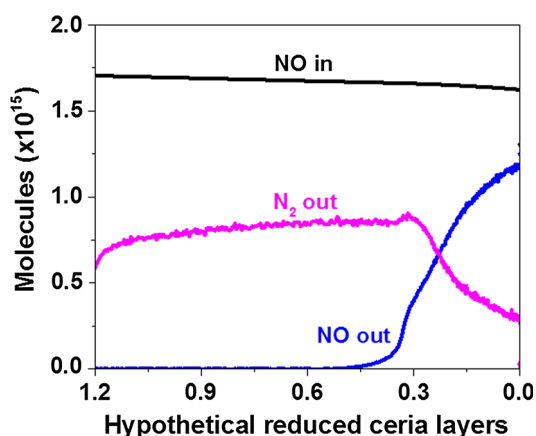


Fig. 5 Reactant and product evolution during NO pulse over CO pre-reduced catalyst at 540 °C

N accumulation (from the N mass balance) is observed and the initially accumulated N is released as N₂ later. Neither N₂O nor NO₂ are observed during this NO titration.

Figure 6 shows the result of the TAP titration experiment with NO over C₃H₆ pre-reduced La–Zr doped ceria at 540 °C. In phase I, corresponding to 1.9–0.5 reduced catalyst layers, the performance is roughly identical to the results obtained for the CO pre-reduced sample: oxygen is accumulated thereby re-oxidizing the catalyst. N₂ is the main observed product while CO or CO₂ are hardly formed. In phase II, the evolution of CO₂ is observed. This evolution of CO₂ is shortly followed by a decrease in the NO conversion. During phase III, NO conversion increases again. In phase IV, NO achieves full conversion, while only N₂ and CO₂ are observed, per 2 NO molecules approximately 1 N₂ and 1 CO₂ molecule are produced. In phase V a progressive decrease in the NO conversion is observed which ceases, when it approaches 0 %. The N₂ and CO₂ production follow the same trend as the NO conversion. The initial absence of oxidation products CO

and CO₂ during the first NO pulses in phase I indicate that the carbonaceous residues left on the surface after C₃H₆ pre-reduction do not directly participate in the reduction of NO into N₂. CO₂ formation is observed until catalyst is re-oxidized to 0.5 reduced layers (phase II). The formation of CO₂ at this point suggests that at a specific catalyst oxidation state the catalyst becomes active for the oxidation of the deposited carbonaceous residues left behind during the C₃H₆ pre-reduction. A temporary NO conversion decrease is observed around the same point of 0.5 reduced layers, the onset of this NO conversion decrease is caused by the depletion of oxygen anion defect sites. The formation of CO₂ proceeds the temporary NO conversion decline. The oxidation of carbonaceous deposits by an oxygen species derived from lattice oxygen to CO₂ (re)creates oxygen anion defect centers capable of NO dissociation into N₂. Therefore, these carbonaceous deposits can be seen as a stored reductant with a delayed function. The presence of the carbonaceous deposits allow for a prolonged period of NO reduction as compared to the CO pre-reduced case. Neither N₂O and NO₂ nor HCN (cyanides) and HNCO (cyanate) are observed during this NO titration.

As TAP is a vacuum technique, in situ Raman (at atmospheric pressure) is applied to confirm the results obtained from TAP. NO reduction is performed over C₃H₆ pre-treated La–Zr doped ceria both at 560 °C and is shown in Fig. 7.

The band at 460 cm^{−1} is attributed to the symmetric stretch mode of Ce–O₈ crystal unit, which is characteristic for the reduced fluorite ceria structure [13]. This peak disappears during the C₃H₆ pre-treatment, while under NO flow the increase in the intensity of the band at 460 cm^{−1} indicates that the pre-reduced La–Zr doped ceria catalyst is re-oxidised by NO. The bands at 1575 and 1350 cm^{−1} are assigned to G band and D band of carbon in the form of graphene or graphite. The G band is usually assigned to zone centre phonons of E_{2g} symmetry of the perfect

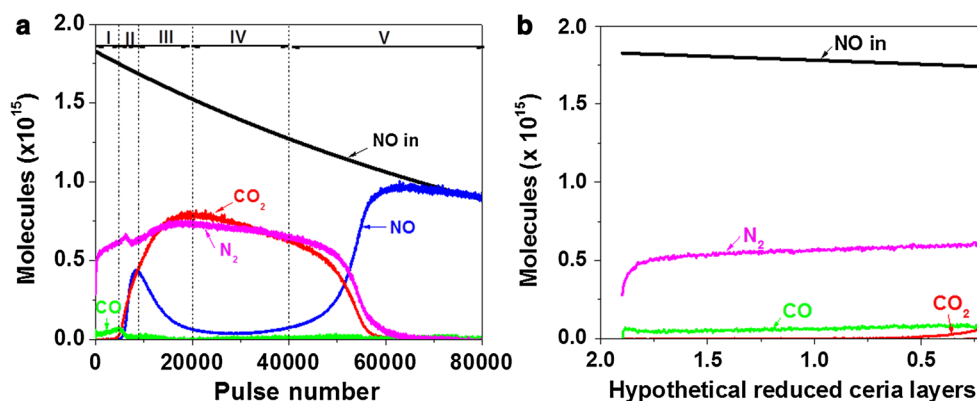


Fig. 6 Reactant and product evolution during NO pulse experiment over C₃H₆ pre-reduced catalyst at 540 °C **a** with pulse number; **b** with number of reduced catalyst layers during phase I of (**a**)

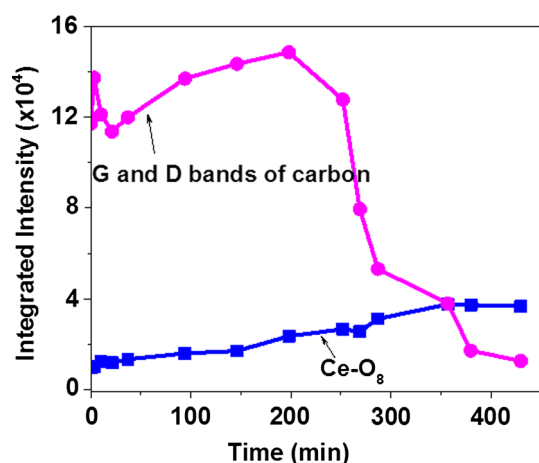


Fig. 7 In-situ Raman experiment. NO reduction over the C_3H_6 pretreated La–Zr doped ceria catalyst at 560 °C, integrated intensity of band(s) at **a** 460 cm^{-1} ; **b** 1575 cm^{-1} (G band) and 1350 cm^{-1} (D band)

graphite structure and the D peak is a breathing mode of A_{1g} symmetry, this mode is forbidden in a perfect graphite structure and only becomes active in the presence of structural defects and disorders [14]. The intensity of D band and G band of graphene/graphite remains constant during the first 270 min of NO/ N_2 flow, this indicates that the oxidation of carbon commences much later than the re-oxidation of the ceria. This observation also points out that the oxidation of carbon is via an oxygen species derived from lattice oxygen and not by gas phase NO, this is in line with previous findings in the oxidation of soot on ceria based catalysts [5].

The inventors of the Di-Air system attribute the exceptional behavior of their catalyst to the formation of cyanate and cyanide type intermediates [2, 3]. In the current study, where the presence of hydrocarbons and NO is decoupled, we find similar exceptional behavior. At 580 °C, hydrocarbon pre-reduced La–Zr doped ceria (21 mg) outperforms CO pre-reduced La–Zr doped ceria by a factor of 13. The amount of extracted oxygen during C_3H_6 is $1.5 \cdot 10^{19}$ atoms and the deposited carbon additionally extracts $3.1 \cdot 10^{19}$ oxygen atoms, which is 13 times more as compared to the amount of extracted oxygen atoms during CO reduction. We find no evidence that hydrocarbon residues or carbonaceous residues play a direct role in NO conversion. These residues, however, allow for a delayed reduction action during lean conditions, where they recreate oxygen anion defects that are responsible for further NO decomposition into N_2 .

3.4 Significance to the Di-Air system

Fuel is used to reduce ceria and, thereby, creating oxygen anion vacancies required for NO decomposition into N_2 . When a fuel injection policy is applied which will keep the

ceria in an partial reduction corresponding to the total reduction state between zero and 0.25 reduced layers, all the oxygen vacancies will be refilled rapidly by the oxidizing gases (NO , CO_2 , O_2 , and H_2O) during this fuel lean condition and there will be no benefit from the delayed reduction action of the deposited carbon. Therefore, a high frequency of fuel injections is required to create locally a rich hydrocarbon environment. When using this fuel injection policy that includes the partial oxidation period (0–2.5 reduced hypothetical ceria layers), the fuel decomposition activity is not only higher, also the carbonaceous deposits act as reductant reservoir and the reduction of the ceria is deeper (up to 2.5 reduction layer). When a fuel pulse has passed and the catalyst is exposed to lean conditions, this deeper reduction degree might be more selective for the NO ceria re-oxidation in competition with O_2 and the other milder oxidizers (CO_2 and H_2O) and once more these carbonaceous deposits keep re-creating lattice oxygen anion vacancies, on which NO can dissociate to form N_2 . Our other work shows NO is able to reduce to N_2 in the presence of excess oxygen [15]. The observed phenomena can have a great impact on the fuel injection policy and the total fuel consumption due to these fuel injections.

4 Conclusion

The hydrocarbon activation activity of the La–Zr doped ceria is limited and requires high temperatures, especially when saturated hydrocarbons will be used. The addition of suitable dopants to the La–Zr doped ceria catalyst is recommended in order to improve its (saturated) hydrocarbon activation capability. Oxygen anion defect centers in the lattice of ceria are responsible for NO decomposition into N_2 , while hydrocarbons deposit carbon species. The oxidation of these deposited carbon species by oxygen species from the lattice can maintain a reduced surface state of the ceria during actual operation under lean conditions, thereby extending the effectiveness of the hydrocarbon injections.

Acknowledgments The authors acknowledge the financial support by the China Scholarship Council (CSC).

Open Access This article is distributed under the terms of the Creative Commons Attribution 4.0 International License (<http://creativecommons.org/licenses/by/4.0/>), which permits unrestricted use, distribution, and reproduction in any medium, provided you give appropriate credit to the original author(s) and the source, provide a link to the Creative Commons license, and indicate if changes were made.

References

1. Bisaiji Y, Yoshida K, Inoue M, Umemoto K, Fukuma T (2012) SAE Int J Fuels Lubr 5:380–388

2. Inoue M, Bisaiji Y, Yoshida K, Takagi N, Fukuma T (2013) *Top Catal* 56:3–4
3. Bisaiji Y, Yoshida K, Inoue M, Takagi N, Fukuma T (2012) *SAE Int J Fuels Lubr* 5:1310–1316
4. Gleaves J, Ebner J, Kuechler T (1988) *Catal Rev* 30:49–116
5. Bueno-López A, Krishna K, Makkee M, Moulijn JA (2005) *J Catal* 230:237–248
6. Yao HC, Yao YFY (1984) *J Catal* 86:254–265
7. Machida M, Murata Y, Kishikawa K, Zhang D, Ikeue K (2008) *Chem Mater* 20:4489–4494
8. Setiabudi A, Chen JL, Mul G, Makkee M, Moulijn JA (2004) *Appl Catal B* 51:9–19
9. Hori CE, Permana H, Ng KS, Brenner A, More K, Rahmoeller KM, Belton D (1998) *Appl Catal B* 16:105–117
10. Sokolovskii V, Buyevskaya O, Plyasova L, Litvak G, Uvarov NP (1990) *Catal Today* 6:489–495
11. Campbell CT, Peden CH (2005) *Science* 309:713–714
12. Zboray M, Bell AT, Iglesia E (2009) *J Phys Chem C* 113:12380–12386
13. Weber W, Hass K, McBride J (1993) *Phys Rev B* 48:178–185
14. Ferrari AC, Robertson J (2000) *Phys Rev B* 61:14095–14107
15. Wang Y, Posthuma de Boer J, Kapteijn F, Makkee M (2016) *ChemCatChem* 8:102–105. doi:[10.1002/cctc.201501038](https://doi.org/10.1002/cctc.201501038)